Control of embryonic stem cell self-renewal and differentiation via coordinated alternative splicing and translation of YY2

Soroush Tahmasebi[a,b,1], Seyed Mehdi Jafarnejad[a,b,1], Ingrid S. Tam[a,b], Thomas Gonatopoulos-Pournatzis[c], Edna Matta-Camacho[a,b], Yoshinori Tsukumo[a,b,2], Akiko Yanagiya[a,b], Wencheng Li[d], Yaser Atlasi[e], Maxime Caron[f,g], Ulrich Braunschweig[c], Dana Pearl[a,b], Arkady Khoutorsky[h], Christos G. Gkogkas[i], Robert Nadon[f,g], Guillaume Bourque[f,g], Xiang-Jiao Yang[a,b,j], Bin Tian[d], Hendrik G. Stunnenberg[e], Yojiro Yamanaka[a,f], Benjamin J. Blencowe[c,k], Vincent Giguère[a,b,j], and Nahum Sonenberg[b,c,3]

[a]Goodman Cancer Research Center, McGill University, Montreal, QC H3A 1A3, Canada; [b]Department of Biochemistry, McGill University, Montreal, QC H3A 1A3, Canada; [c]Donnelly Centre, University of Toronto, Toronto, ON M5S 3E1, Canada; [d]Department of Microbiology, Biochemistry, and Molecular Genetics, Rutgers New Jersey Medical School, Newark, NJ 07103; [e]Department of Molecular Biology, Faculty of Science, Radboud University, Nijmegen, 6525GA, The Netherlands; [f]Department of Human Genetics, McGill University, Montreal, QC H3A 1A3, Canada; [g]McGill University and Genome Quebec Innovation Centre, Montreal, QC H3A 0G1, Canada; [h]Department of Anesthesia, McGill University, Montreal, QC, H3G 1Y6, Canada; [i]Patrick Wild Centre, Centre for Integrative Physiology, University of Edinburgh, Edinburgh, EH8 9XD, United Kingdom; [j]Department of Medicine, McGill University Health Center, Montreal, QC H3A 1A3, Canada; and [k]Department of Molecular Genetics, University of Toronto, Toronto, ON M5S 1A8, Canada

This contribution is part of the special series of Inaugural Articles by members of the National Academy of Sciences elected in 2015.

Contributed by Nahum Sonenberg, September 22, 2016 (sent for review August 15, 2016; reviewed by George Q. Daley and Maurice S. Swanson)

Translational control of gene expression plays a key role during the early phases of embryonic development. Here we describe a transcriptional regulator of mouse embryonic stem cells (mESCs), Yin-yang 2 (YY2), that is controlled by the translation inhibitors, Eukaryotic initiation factor 4E-binding proteins (4E-BPs). YY2 plays a critical role in regulating mESC functions through control of key pluripotency factors, including Octamer-binding protein 4 (*Oct4*) and Estrogen-related receptor-β (*Esrrb*). Importantly, overexpression of YY2 directs the differentiation of mESCs into cardiovascular lineages. We show that the splicing regulator Polypyrimidine tract-binding protein 1 (PTBP1) promotes the retention of an intron in the 5′-UTR of *Yy2* mRNA that confers sensitivity to 4E-BP–mediated translational suppression. Thus, we conclude that YY2 is a major regulator of mESC self-renewal and lineage commitment and document a multilayer regulatory mechanism that controls its expression.

mRNA translation | 4E-BPs | PTBP | embryonic stem cell | YY2

Stringent control of mRNA translation is critical during early embryonic development, because relatively small changes in the expression of development-related genes can dramatically affect the self-renewal and differentiation of stem cells. In fact, a modest (twofold or less) increase or decrease in Octamer-binding protein 4 (OCT4) or Sex-determining region Y (SRY)-box 2 (SOX2) protein levels impairs ESC self-renewal and triggers differentiation (1, 2). mRNA translation, which is low in undifferentiated embryonic stem cells (ESCs) and multipotent somatic stem cells (e.g., hematopoietic stem cells and skin stem cells), increases significantly during differentiation (3–5). Importantly, genome-wide analysis of the transcriptome vs. proteome of ESCs during the early stages of differentiation demonstrated that protein levels correlate poorly with mRNA levels (Pearson's $R < 0.4$), underscoring the importance of posttranscriptional regulation in ESC differentiation (6).

mRNA translation can be divided into three steps: initiation, elongation, and termination. Translational control has been documented most extensively at the initiation step, at which ribosomes are recruited to the mRNA by the concerted action of Eukaryotic translation initiation factors (eIFs) (7). Control of translation is exerted mainly by two key protein complexes: eIF4F (eIF4E–eIF4G–eIF4A) and the ternary complex (eIF2–GTP–Met-tRNA$^{Met}_i$) (7). The mammalian target of rapamycin complex 1 (mTORC1) controls the assembly of eIF4F through the phosphorylation of eIF4E-binding proteins (4E-BPs) (8, 9). The 4E-BPs consist of a family of small molecular weight (15–20 kDa) translational inhibitors (4E-BP1, -2, and -3 in mammals), that, when dephosphorylated, avidly bind eIF4E and block its association with eIF4G to form the eIF4F complex. Following phosphorylation by mTORC1, 4E-BPs dissociate from eIF4E, allowing the formation of the eIF4F complex and activation of translation (8, 10–12). 4E-BPs inhibit cap-dependent translation in embryonic and somatic stem cells (3, 4, 13, 14). Although eIF4E promotes cap-dependent translation of all cellular mRNAs, the translation of a subset of mRNAs, which generally contain a long and highly structured 5′-UTR, is strongly dependent on eIF4E (9, 15). These mRNAs are known as "eIF4E-sensitive" and

Significance

Embryonic stem cells (ESCs) maintain a low translation rate; therefore control of mRNA translation is critical for preserving their stemness. We identified a hitherto unstudied transcription factor, Yin-yang 2 (YY2), which is translationaly regulated and controls self-renewal and differentiation of mouse ESCs (mESCs). Although YY2 is essential for mESC self-renewal, increased YY2 expression directs differentiation of mESCs toward cardiovascular lineages. Examination of the *Yy2* 5′-UTR revealed a multilayer regulatory mechanism through which YY2 expression is dictated by the combined actions of the splicing regulator, Polypyrimidine tract-binding protein 1 (PTBP1), and the translation inhibitors, Eukaryotic initiation factor 4E-binding proteins (4E-BPs). YY2 directly controls the expression of several pluripotency and development-related genes. This study describes a synchronized network of alternative splicing and mRNA translation in controlling self-renewal and differentiation.

Author contributions: S.T., S.M.J., and N.S. designed research; S.T., S.M.J., I.S.T., T.G.-P., E.M.-C., Y.T., A.Y., W.L., D.P., A.K., X.-J.Y., and Y.Y. performed research; C.G.G. contributed new reagents/analytic tools; S.T., S.M.J., I.S.T., T.G.-P., E.M.-C., Y.T., A.Y., W.L., Y.A., M.C., U.B., R.N., G.B., B.T., H.G.S., Y.Y., B.J.B., and V.G. analyzed data; and S.T., S.M.J., and N.S. wrote the paper.

Reviewers: G.Q.D., Children's Hospital Boston; and M.S.S., University of Florida.

The authors declare no conflict of interest.

[1]S.T. and S.M.J. contributed equally to this article.

[2]Present address: Division of Molecular Target and Gene Therapy Products, National Institute of Health Sciences, Setagaya-ku, Tokyo 158-8501, Japan.

[3]To whom correspondence should be addressed. Email: nahum.sonenberg@mcgill.ca.

This article contains supporting information online at www.pnas.org/lookup/suppl/doi:10.1073/pnas.1615540113/-/DCSupplemental.

encode proteins that control fundamental cellular processes such as cell proliferation and survival (16).

We showed that 4E-BPs are required for reprogramming mouse embryonic fibroblasts (MEFs) to induced pluripotent stem cells (iPSCs) (17). In the current study, we describe a tightly coordinated network in mESCs whereby the expression of the Yin-yang 2 (YY2) transcription factor is controlled by the splicing regulator Polypyrimidine tract-binding protein 1 (PTBP1) and the 4E-BP translation inhibitors. Our data reveal that stringent regulation of YY2 expression by this network is critical for mESC self-renewal and lineage commitment.

Results

Transcriptome and Translatome Profiling of WT and 4E-BP1/2–Null mESCs. To investigate the role of 4E-BPs in mESCs, we first derived mESCs from WT and Eukaryotic translation initiation factor 4E-binding protein 1 (*Eif4ebp1*) and Eukaryotic translation initiation factor 4E-binding protein 2 (*Eif4ebp2*) double-knockout (DKO) mice and then examined the eIF4F complex using a 7-methyl-GTP (m^7GTP)-agarose pull-down assay. The eIF4F amount was elevated, as demonstrated by increased (~10.6-fold) eIF4G1 pull-down in DKO mESCs (Fig. S1*A*). However, polysome profiling (Fig. S1*B*) and [^{35}S]methionine/cysteine-labeling assays (Fig. S1*C*) did not detect a substantial difference in global mRNA translation between WT and DKO mESCs. These data are consistent with previous findings that the lack of 4E-BPs affects the translation of a subset of mRNAs rather than affecting global translation (17, 18).

To identify 4E-BP–sensitive mRNAs in mESCs, we performed ribosome profiling (19), which allows precise measurement of the translation of mRNAs on a genome-wide scale, by deep sequencing of ribosome-protected fragments (ribosome footprints; RFPs). We achieved a high degree of reproducibility between the replicates for mRNA sequencing (mRNA-Seq) and RFPs ($R^2 > 0.97$, Fig. S1*D*). Metagene analysis confirmed the enrichment of RFP reads in coding sequences and the expected three-nucleotide periodicity (Fig. S1*E*). These analyses validated the quality of the mRNA and RFP libraries (Table S1). We used Babel analysis (20) to compute changes in the abundance of RFPs (Fig. 1*A*) independent of changes in the levels of their corresponding mRNAs (Fig. 1*B*). A significant enhancement in the translation efficiency of a small subset of mRNAs was detected in DKO mESCs [false discovery rate (FDR) < 0.1] (Fig. 1*C* and Dataset S1), as is consistent with the lack of global change in translation in the DKO mESCs (Fig. S1 *B* and *C*). Strikingly, mRNA-Seq data revealed down-regulation of mRNA levels for several pluripotency factors, such as PR domain-containing 14 (*Prdm14*), ES cell-expressed Ras (*Eras*), Estrogen-related receptor-β (*Esrrb*), and *Nanog* (−1.3, −1, −0.6, and −0.9, respectively; $\log_2$ DKO/WT) in DKO mESCs (Dataset S2). Possible reasons for this down-regulation are discussed below.

Ablation of *Eif4ebp1* and *Eif4ebp2* Results in Reduced Expression of mESC Markers. To validate the mRNA-Seq results, we examined the expression of pluripotency factors in undifferentiated WT and DKO mESCs, and also in WT and DKO mESCs after differentiation, by Western blot and quantitative RT-PCR (RT-qPCR). Although all DKO mESC lines maintained normal morphology under standard mESC culture conditions [in the presence of Leukemia inhibitory factor (LIF) and feeder layer (irradiated MEFs)], expression of the ESC marker NANOG was reduced by 60–70% (Fig. 1*D*). These changes did not result from unintended consequences of the knockout procedure, because RNAi-mediated depletion of 4E-BP1 and -2 (double knockdown; DKD) resulted in a strong (80%) reduction in NANOG (Fig. S2*A*). DKO mESCs proliferated more slowly than WT mESCs (Fig. S2*B*), and when cultured in the absence of feeder layer, they exhibited flattened morphology, which is indicative of cellular differentiation, whereas WT mESCs preserved their normal morphology (Fig. S2*C*). Similar morphological changes were observed in DKD ESCs (Fig. S2*D*). Notably, when cultured in the absence of LIF and a feeder layer, NANOG and OCT4 expression was strongly suppressed in DKO mESCs, whereas WT mESCs maintained a higher expression of these proteins (Fig. S2*E*). In addition to *Nanog*, mRNA levels of *Oct4* and *Sox2* were lower in DKO mESCs on day 0 of differentiation (Fig. S2*F*). Moreover, as determined by RT-qPCR, mRNA levels of several other ESC factors, such as *Lin28a*, *Eras*, and ten-eleven translocations (*Tets*) (*Tet1*, *-2*, and *-3*), were reduced in DKO mESCs (Fig. S2*G*). Therefore, 4E-BPs are required for the regulation of expression of pluripotency factors. Analysis of embryoid bodies (EBs) derived from WT and DKO ESCs revealed that the lack of 4E-BP1 and 4E-BP2 resulted in the differentiation of mESCs toward mesodermal and endodermal lineages, as indicated by significant up-regulation of Bone morphogenetic protein 4 (*Bmp4*), an early mesoderm marker, and *Gata4* and *Gata6*, early endoderm markers (Fig. S2*H*). This up-regulation coincides with the down-regulation of the neuroectoderm markers Microtubule-associated protein 2 (*Map2*) and Sex-determining region Y (SRY)-box 17 (*Sox17*) mRNAs in DKO EBs.

The decrease in mRNA levels for several pluripotency factors, such as *Nanog*, *Eras*, and *Esrrb* in DKO mESCs compared with WT mESCs (Fig. 1*D*, Fig. S2 *F* and *G*, and Dataset S2) suggests that 4E-BP–dependent translational regulation of one or more factor(s) affects these changes in the transcriptome.

Stringent Control of YY2 Expression in mESCs. One of the mRNAs exhibiting the most significant increase in translation efficiency in DKO mESCs versus WT cells is the *Yy2* transcription factor (Babel *P* value = 0.0001) (Fig. 1*C* and Dataset S1). YY2 exhibits considerable sequence homology (56% identity) with the YY1 transcription factor (21). Like reduced expression 1 (Rex1) [Zinc finger protein 42 (Zfp42)], a well-known ESC marker (22, 23),

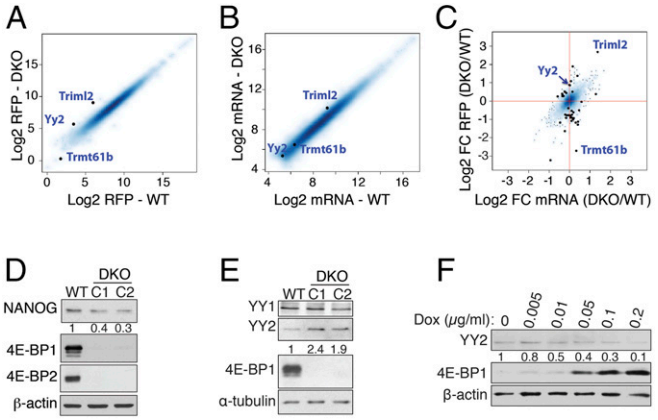

Fig. 1. The lack of 4E-BPs deregulates the expression of pluripotency factors in mESCs. (*A* and *B*) The $\log_2$ abundance of RFPs (*A*) and mRNA (RNA-Seq) (*B*) of transcripts that were included in Babel analysis are plotted for WT and *Eif4ebp1* and *Eif4ebp2* DKO mESCs. (*C*) Babel analysis of transcripts with a significant change in RFPs independent of the corresponding change in mRNA abundance (black dots; FDR < 0.1). *Triml2* and *Trmt61b*, respectively, are mRNAs with the highest and the lowest RFP ratios in DKO compared with WT mESCs; FC, fold change. (*D*) Western blot analysis of NANOG expression in a WT mESC and in two independent DKO mESC clones (C1 and C2). Numbers indicate the ratio of NANOG expression in each clone to that in the WT mESC followed by normalization with β-actin. (*E*) Western blot analysis of YY2 and YY1 expression in a WT mESC and two independent DKO mESC clones. Numbers indicate the ratio of YY2 expression in each clone compared with the WT mESC followed by normalization with α-tubulin. (*F*) DKO mESCs carrying the doxycycline-inducible 4E-BP1-4A mutant construct were treated with 0, 0.005, 0.01, 0.05, 0.1, or 0.2 μg/mL doxycycline for 24 h and were subjected to Western blot analysis. Numbers indicate the ratio of YY2 expression in each treatment compared with no doxycycline followed by normalization with β-actin.

YY2 is a retroposed copy of the YY1 gene, which evolved only in placental mammals (24). YY1 is a pleiotropic transcription factor that regulates diverse cellular processes and plays a critical role in early embryonic development, ESC biology, and reprogramming (25–27). Although the N-terminal domains of YY1 and YY2 differ significantly, the C-terminal DNA-binding domain of YY1 is highly conserved in Rex1 and YY2 (22), suggesting that YY2 may play an important role in the regulation of gene expression in mESCs. Although there is no significant change in the level of *Yy2* mRNA in DKO mESCs compared with WT cells (Fig. S3*A*), YY2 protein, but not YY1, is elevated 1.9- to 2.4-fold in DKO mESCs (Fig. 1*E*). Importantly, expression of a phosphorylation-resistant 4E-BP1-4A mutant (28) in DKO mESCs reduced YY2 protein levels (Fig. 1*F*). These data demonstrate that translation of *Yy2* mRNA is controlled by 4E-BPs.

To study the functional consequence of YY2 up-regulation in mESCs, we generated an mESC line carrying a doxycycline-inducible YY2 construct (dox-YY2). Overexpression of YY2 caused a reduction in the expression of pluripotency factors *Nanog*, *c-Myc*, and *Oct4* mRNAs (Fig. 2 *A* and *B*), indicating a negative role for YY2 in mESC self-renewal. However, constitutively expressed shRNA against *Yy2* in mESCs caused depletion of mESCs in culture (Fig. S3*B*). This depletion coincided with increased levels (8.4- ± 2.4-fold) of the apoptosis marker, cleaved caspase-3, in *Yy2*-knockdown cells (Fig. S3*C*), suggesting that mESCs require a basal level of YY2 expression for survival. To study the impact of a moderate knockdown, we generated an mESC line carrying a doxycycline-inducible shRNA construct against *Yy2* (shYy2). Although slight induction of shYy2 (0.2 μg/mL doxycycline) enhanced expression of the pluripotency factors *Nanog* and *Sox2* (Fig. 2*C*), higher doses of doxycycline failed to do so (Fig. 2*C*), indicating a dose-sensitive effect of YY2 on the expression of mESC pluripotency factors. Importantly, the deleterious effect of complete depletion of YY2 was not limited to mESCs, because CRISPR/Cas9-mediated *Yy2*-knockout blastocysts were unable to maintain their inner cell mass, as demonstrated by blastocyst outgrowth assays (Fig. 2*D* and Fig. S3 *D* and *E*). A similar defective outgrowth has been described previously for $Yy1^{-/-}$ blastocysts (29), suggesting that the lack of YY2 may cause peri-implantation lethality, as described for $Yy1^{-/-}$ mice (26), and demonstrating that YY1 and YY2 fulfill nonredundant functions in blastocyst growth.

Recent studies showing that YY1 directly regulates Nkx2.5 expression and promotes cardiogenesis uncovered a novel function for YY1 in cardiomyocyte differentiation and cardiac morphogenesis (30, 31). To examine the effect of YY2 on mESC differentiation toward cardiovascular lineages, EBs derived from dox-YY2 mESCs were exposed to doxycycline. One week after induction of YY2 expression, foci of beating cardiomyocytes began to appear in the plates with the highest level of YY2 induction (0.2 μg/mL doxycycline) (Movie S1), and the number of foci continued to increase during the following 2 weeks. No beating foci appeared in noninduced EBs up to the third week of differentiation. Consistently, expression of several cardiovascular-specific markers, such as *Nkx2.5*, Bone natriuretic peptide (*Bnp*), alpha-Myosin heavy chain (*αMHC*), Myosin light chain 2a (*MLC2a*), and *MLC2v* mRNAs was increased in the YY2-overexpressing EBs in a dose-dependent manner (Fig. 2*E*). These data suggest that YY1 and YY2 have overlapping functions in directing the differentiation of mESC toward cardiovascular lineages.

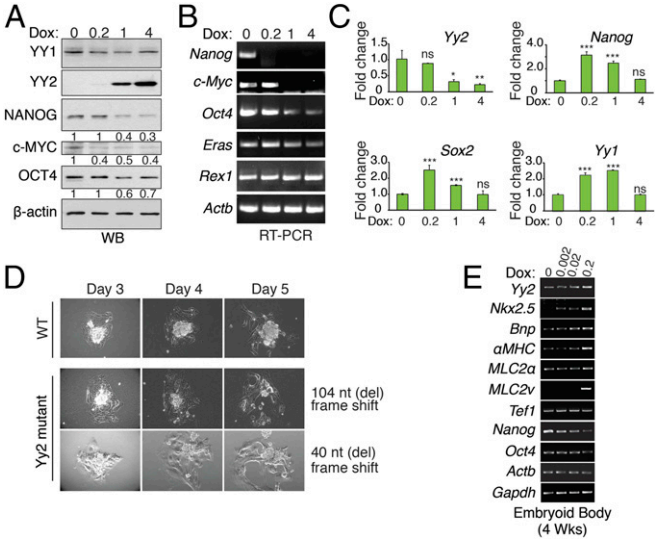

Fig. 2. Stringent regulation of YY2 levels is critical for mESC survival and differentiation. (*A* and *B*) Western blot (*A*) and RT-PCR (*B*) analysis of WT mESCs carrying the doxycycline-inducible YY2 construct and treated with 0, 0.2, 1, or 4 μg/mL doxycycline for 24 h. Numbers indicate the ratio of the expression of the identified protein in each treatment compared with no doxycycline followed by normalization with β-actin. (*C*) RT-qPCR analysis of mESCs carrying doxycycline-inducible shRNA against *Yy2* (shYy2) and treated with doxycycline (0, 0.2, 1, or 4 $\mu g \cdot mL^{-1} \cdot d^{-1}$) for 72 h. Values are normalized to *β-actin*. Data are mean ± SD ($n = 3$). *$P < 0.05$, **$P < 0.01$, ***$P < 0.001$; ns, nonsignificant. (*D*) Blastocyst outgrowth assay in a WT embryo and in two independent CRISPR/CAS9-mediated *Yy2*-knockout embryos. Cas9 mRNA and sgRNAs targeting *Yy2* were injected into zygotes. The blastocysts derived from injected embryos were subjected to the blastocyst outgrowth assay. The mutagenesis strategy and the sequence of mutant alleles are provided in Fig. S3 *D* and *E*. (*E*) RT-PCR analysis of EBs carrying the doxycycline-inducible YY2 construct and treated with 0, 0.002, 0.02, or 0.2 μg/mL doxycycline every other day for 4 wk.

YY2 Binds to the Regulatory Regions of Key Genes for ESC Pluripotency and Differentiation. Genomic targets of YY1, but not YY2, in mESCs have been documented (25, 32). We determined the genome-wide binding sites of YY2 in mESCs by ChIP-Seq in WT mESC cells overexpressing YY2. Because of the high degree of similarity between the C-terminal domains of YY1 and YY2, we used a monoclonal antibody that specifically recognizes the N-terminal domain of YY2 (Fig. 2*A* and Fig. S3*F*; also see *SI Materials and Methods*). YY2-binding sites (Dataset S3) exhibit enrichment for the genomic loci of coding genes (exons or introns, indicated by gene, 43%) (Fig. 3*A*) and a preference for the promoter regions surrounding the transcription start sites (TSS) (Fig. 3*B*). Nearly half of the peaks contained the consensus YY1-binding motif (Fig. 3*C*), as is consistent with a similar sequence preference for YY1 and YY2 (21, 22). Motif distribution across binding peaks revealed enrichment for the known consensus YY1-binding motif directly at YY2 peak centers (Fig. 3*D*), indicating specific recognition of these binding sites by YY2.

Pathway analysis of genes associated with YY2-binding peaks using the Ingenuity Pathway Analysis (IPA) program revealed significant enrichment for genes related to ESC pluripotency (Fig. 3*E*), such as *Oct4*, Teratocarcinoma-derived growth factor 1 (*Tdgf1*), *Esrrb*, and Forkhead box protein D3 (*FoxD3*). We also found enrichment for genes involved in the activation of the retinoic acid receptor (RAR)-signaling pathway. Previous studies showed that activation of the RAR pathway promotes differentiation of ESCs to cardiomyocytes, particularly $MLC2v^{+}$ ventricular cardiomyocytes, and that the RAR-signaling pathway plays a critical role in cardiogenesis (33, 34). These findings indicate that activation of this pathway, along with other cardiovascular-related YY2 targets [e.g., *Bnp*, Mesoderm posterior protein 2 (*Mesp2*), and MKL (megakaryoblastic leukemia)/myocardin-like 1 (*Mkl1*)], is responsible for engendering the differentiation of mESCs toward the cardiovascular lineage by YY2 (Fig. 2*E*). We validated the ChIP-Seq results for a selected number of genes with ChIP-qPCR (Fig. 3 *F* and *G* and Fig. S3*G*).

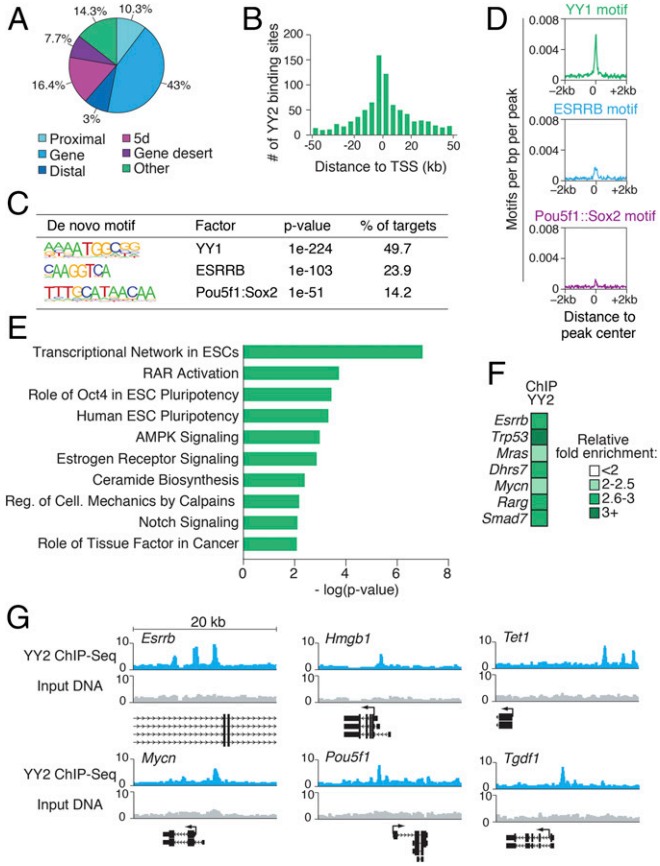

Fig. 3. YY2 controls the ESC transcriptional regulatory network and development-related genes. (*A*) Pie chart displaying the distribution of YY2 ChIP-Seq peaks across the genome based on the distance of the peaks from the nearest RefSeq gene: proximal, <2 kb upstream of the TSS; gene, exon or intron; distal, 2–10 kb upstream of the TSS; 5d, 10–100 kb upstream of the TSS; gene desert, >100 kb from a RefSeq gene; and other, anything not included in the above categories. (*B*) Histogram depicting the distance of YY2 ChIP-Seq peaks relative to the TSS of the nearest gene. (*C*) De novo motifs enriched in YY2-binding events. Enrichment *P* values and percentage of targets containing each motif are displayed, as generated by HOMER software. (*D*) Plots showing the average density of selected motifs in a window 2 kb from the YY2 peak center. (*E*) The most significantly enriched canonical pathways in genes associated with YY2 ChIP-Seq peaks, as identified by IPA. (*F*) Standard ChIP-qPCR validation of YY2-binding regions. Data are normalized to IgG. The *Lmnb2* gene was used as a negative control. (*G*) Graphical representation of selected YY2-binding peaks, obtained from the University of California, Santa Cruz (UCSC) browser. Twenty-kilobase windows are displayed.

RT-qPCR analysis of a selected number of pluripotency factors in the ChIP-Seq dataset, such as *Oct4*, *Esrrb*, *Tet1*, and *Tet2* mRNAs, revealed that YY2 overexpression suppresses their expression in mESCs (Fig. 4*A*). The ChIP-Seq analysis did not identify *Nanog* as a target of YY2. Thus, the decrease in *Nanog* mRNA expression in DKO mESCs (Dataset S2) or upon overexpression of YY2 (Fig. 2 *A* and *B*) is likely secondary to the down-regulation of other pluripotency factors. In agreement with our previous observation (Fig. 2*C*), doxycycline-inducible *Yy2* knockdown in mESCs revealed a dose-sensitive regulation of its target genes (Fig. 4*B*).

We analyzed the target genes identified by the YY2 ChIP-Seq assay relative to those of YY1 in mESCs (32) and found that 27.7% of YY2 targets are shared with YY1 (Fig. 4*C* and Dataset S3). Conversely, a large portion of the YY2 targets (~72%) are not present among the YY1 targets (Fig. 4*C*), a finding that supports a previous study of genome-wide mRNA expression in HeLa cells demonstrating that YY1 and YY2 regulate some shared but mostly unique sets of genes (35). Although some pluripotency-related genes such as *Tdgf1* are unique YY2 targets, *Oct4*, Krüppel-like factor 5 (*Klf5*), and *Foxd3* are common targets of YY1 and YY2 (Fig. 4*C*). Notably, *Yy1* is a target of both YY1 and YY2, and our data showed that YY2 has a dose-sensitive effect on YY1 expression (Fig. 2 *A* and *C*). The similar consensus-binding motifs of YY1 and YY2 are consistent with these factors exhibiting overlapping or competing effects on common target genes (21, 36–38). One plausible explanation for their distinct activities is the considerable divergence in their N-terminal domains (Fig. S4*A*). A recent report showed that the binding of YY1 to active promoters/enhancers in ESCs through its C-terminal DNA-binding domain is facilitated by concurrent binding of its N-terminal domain to RNA species transcribed from these regulatory elements (32). We hypothesized that the N-terminal domain of YY2 cannot interact with RNA. We examined this possibility by EMSA using purified mouse YY1 and YY2 proteins (Fig. S4 *B* and *C*) and DNA and RNA probes derived from the AT-rich interactive domain-containing protein A1 (*ARID1A*) promoter, which interact with YY1 (32). Notably, *Arid1a* is among the YY2 targets in our ChIP-Seq analysis (Dataset S3). Although YY2 interacts with the DNA probe with only slightly less efficiency than YY1 (Fig. 4*D*), only YY1 binds to the RNA probe (Fig. 4*E*), because no visible binding to the *Arid1a*

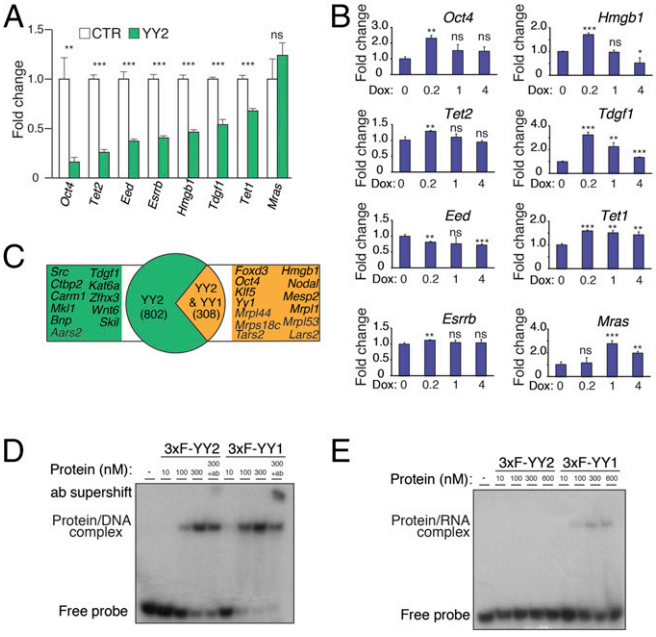

Fig. 4. The regulatory network and distinct mode of action of YY2 compared with YY1. (*A*) RT-qPCR analysis of selected YY2 targets in control and YY2-overexpressing mESCs. mESCs carrying the doxycycline-inducible YY2 construct were treated with 0 or 0.2 μg/mL doxycycline for 24 h. Values are normalized to *β-actin*. Data are mean ± SD (n = 3). $^{**}P < 0.01$, $^{***}P < 0.001$; ns, nonsignificant. (*B*) RT-qPCR analysis of YY2 targets in mESCs carrying a doxycycline-inducible shYy2 and treated with doxycycline as described in Fig. 2*C*. Values are normalized to *β-actin*. Data are mean ± SD (n = 3). $^{*}P < 0.05$, $^{**}P < 0.01$, $^{***}P < 0.001$; ns, nonsignificant. (*C*) Comparison of YY2 and YY1 ChIP-Seq targets in mESCs. Only peaks with at least a 1-nt overlap were considered as common targets. (*D*) EMSA with a radioactive-labeled dsDNA oligonucleotide probe derived from the promoter region of the mouse *Arid1a* gene (32) and purified recombinant mouse triple Flag-tagged (3xF)-YY1 and 3xF-YY2 proteins. The probes were incubated in the presence of increasing amounts of recombinant proteins and in the presence or absence of antibodies as indicated. (*E*) EMSA with a radioactively labeled single-stranded RNA oligonucleotide probe derived from the promoter region of the mouse *Arid1a* gene (32) and purified recombinant mouse 3xF-YY1 and 3xF-YY2 proteins.

promoter-derived RNA was detected for YY2, even after prolonged exposure (Fig. S4*D*). In agreement with these results, analysis of the N-terminal domains of mouse YY1 and YY2 proteins by BindN, an RNA-binding prediction server (39), identified two distinct RNA-binding motifs for YY1 that are not conserved in YY2 (Fig. S4*E*). Our data suggest a mechanism by which YY2 may act differently from YY1 and that their differential affinity for the promoter-derived RNAs underlies the opposing effects of YY1 and YY2 on certain shared promoters.

A Retained 5′-UTR Intron Renders *Yy2* mRNA Sensitive to 4E-BP–Dependent Translational Repression. To search for eIF4E-sensitive elements in the 5′-UTR of *Yy2* mRNA, we first used 5′-RACE to annotate the sequence in mESCs. In addition to the annotated mRNA sequence of the 217-nt 5′-UTR (RefSeq: NM_001098723.1), henceforth referred to as "variant A," we uncovered two additional variants possessing 290-nt and 100-nt 5′-UTRs, respectively (Fig. 5 *A* and *B*). The 290-nt variant (designated "variant B") is a 5′ extension of variant A; the 100-nt variant is a spliced version of variant A, lacking 117 nucleotides. The spliced region harbors all the features of a canonical intron, including a GU dinucleotide at the 5′ splice site (SS), an AG dinucleotide at the 3′ SS, and a polypyrimidine tract and putative branch site A nucleotide within 20 nt of the 3′ SS (Fig. 5*A*). Considering that the intronic sequence is shared between variants A and B, we termed their corresponding spliced variants ΔA and ΔB, respectively (Fig. 5*B*). Retroposed genes are generally intronless, because they are generated through the reverse transcription of mature mRNAs (40, 41). Therefore, the intron acquisition by *Yy2* is most likely a recent evolutionary event that occurred after the retroposition of *Yy2* from *Yy1* in placental mammals.

To measure intron retention in *Yy2* mRNA during differentiation of mESCs by RT-PCR, we used two forward primers (Fw1 and Fw2) and a common reverse primer (Rv) to target the flanking exons (Table S2). Primers Fw1 and Rv detect only variants B and ΔB (297-bp and 180-bp PCR products, respectively), whereas Fw2 and Rv amplify a 209-bp PCR product for variants A and B and a 92-bp PCR product for variants ΔA and ΔB. We examined Yy2 intron retention events in mESCs and EBs at days 4 and 6 postdifferentiation and measured the degree of intron retention using the percent intron retention (PIR) as a metric (42). The percentage of nonspliced variants (A and B) is higher in mESCs than in EBs, demonstrating that differentiation coincided with a marked reduction in intron retention (Figs. 5*C* and Fig. S5*A*). Notably, this alternative splicing event is not restricted to mESCs, because various degrees of intron retention were detected at different embryonic stages and across different tissues (Fig. 5*D* and Fig. S5*B*), demonstrating developmental and tissue-specific regulation of *Yy2* alternative splicing.

To identify the *trans*-acting factor(s) responsible for *Yy2* alternative splicing, we used the RBPmap web server to predict consensus motifs for RNA-binding proteins (43). We identified two canonical PTBP recognition motifs (CUCUCU) flanking the *Yy2* 5′-UTR intron (Fig. 5 *A* and *B* and Fig. S5*C*). PTBP1 and PTBP2 (a neural- and testis-enriched paralog) are RNA-binding proteins implicated in several aspects of mRNA metabolism, including alternative splicing, stability, localization, and polyadenylation (44). PTBP1 is essential for embryonic growth before gastrulation, because *Ptbp1*$^{-/-}$ mESCs have severe proliferation defects (45, 46). To explore its role in *Yy2* 5′-UTR intron retention, PTBP1 was depleted in mESCs using shRNA (Fig. S5*D*). PTBP1 knockdown resulted in reduced *Yy2* intron retention, demonstrating that it acts as an inhibitor of *Yy2* splicing in mESCs (Fig. 5*E*). This knockdown was associated with reduced growth and smaller colonies of mESCs (Fig. S5*E*). To demonstrate that PTBP1 directly affects *Yy2* 5′-UTR splicing, we

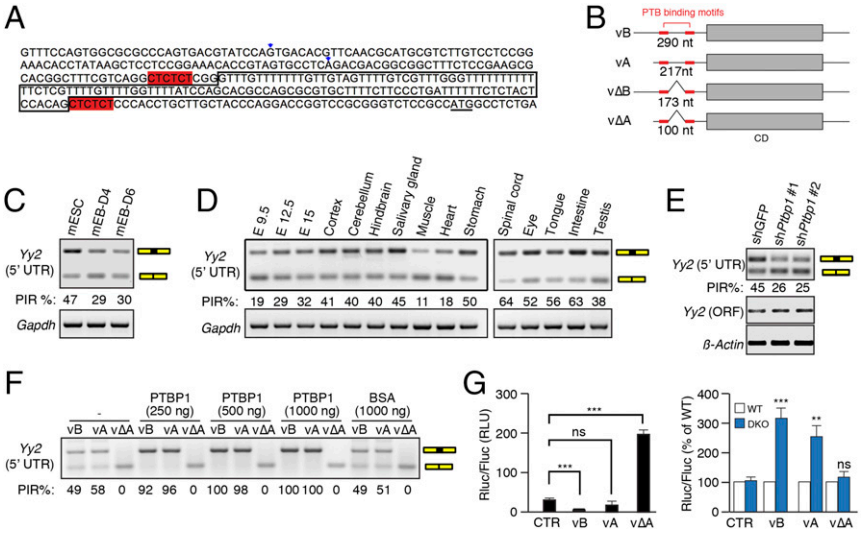

Fig. 5. Retention of the 5′-UTR intron renders *Yy2* sensitive to 4E-BP–mediated translation suppression. (*A*) Sequence of the promoter region of the mouse *Yy2* gene. The two alternative TSS are marked by arrowheads; the boxed sequence shows the retained intron; the two hexamers highlighted in red are the consensus PTBP-binding motifs; and the underlined ATG is the translation start codon for *Yy2* mRNA. (*B*) A cartoon depicting the four variants of *Yy2* 5′-UTR. vB and vΔB represent a long variant with and without intron retention, respectively; vA and vΔA represent a short variant with and without intron retention, respectively. CD, coding DNA sequence. (*C*) RT-PCR using the primer pair Fw2 and Rv designed to recognize all four possible variants to estimate the splicing efficiency of the 5′-UTR intron in mESCs and mEBs on days 4 and 6 postdifferentiation. *Gapdh* mRNA was used as the control. (*D*) RT-PCR analysis of intron retention (IR) in the *Yy2* 5′-UTR in different mouse embryonic stages and adult tissues using the primers described in *C*. *Gapdh* mRNA was used as the control. (*E*) RT-PCR analysis of intron retention in the *Yy2* 5′-UTR using the primers described in *C* upon depletion of PTBP1 expression in mESCs by two independent shRNAs. *Yy2*-ORF primers amplifying a segment of the coding region of *Yy2* transcript were used to demonstrate the change in overall expression of *Yy2* mRNA. *β-actin* mRNA was used as the internal control. (*F*) RT-PCR amplification (primers Fw2 and Rv) of the in vitro splicing products of the A, B, and ΔA variants in WERI retinoblastoma cell extracts with different amounts of recombinant PTBP1 protein. Recombinant BSA was used as a negative control. (*G*) Luciferase reporter assay with Firefly (Fluc) and *Renilla* (Rluc) luciferase reporter mRNAs, as described in Fig. S5*J*. The in vitro-transcribed mRNAs were purified and transfected into WT and DKO mESCs. (*Left*) The normalized luciferase activity of each construct in WT mESCs. (*Right*) Comparison of the luciferase activity of each construct in DKO and WT mESCs. *Fluc* mRNA was cotransfected with *Rluc* mRNA as a transfection control. Data are mean ± SD (n = 3). $^{**}P < 0.01$, $^{***}P < 0.001$; ns, nonsignificant. CTR, control; RLU, relative luminescence units.

performed an in vitro splicing assay using a WERI retinoblastoma (WERI-Rb1) cell extract, purified recombinant PTBP1 protein, and the three *Yy2* 5′-UTR variants (A, B, and ΔA) transcribed in vitro. Incubation in the cell extract resulted in splicing of the introns from A and B variants but had no effect on the ΔA variant (Fig. S5 *F* and *G*). Importantly, the addition of recombinant PTBP1 protein (Fig. S5*H*) dramatically suppressed splicing and resulted in the complete retention of the intron in a dose-dependent manner (Fig. 5*F* and Fig. S5*I*).

The length and complexity of the 5′-UTR play a critical role in mRNA translation, because mRNAs with long and structured 5′-UTRs are more sensitive to eIF4E activity (15, 47). The combined use of alternative TSS and alternative splicing determine the complexity of the *Yy2* 5′-UTR. To examine the effect of 5′-UTR variants on mRNA translation, we constructed luciferase reporters containing the 5′-UTRs of the A, B, and ΔA variants (Fig. S5*J*) and used the reporters to generate mRNAs that were transfected into WT and DKO mESCs. The B, and to a lesser extent A, variant mRNAs were poorly translated, whereas translation of the intron-less ΔA variant was markedly more efficient (more than sixfold higher than control) in WT mESCs (Fig. 5*G*, *Left*). These data demonstrate that the 5′-UTR containing the retained intron sequence inhibits translation. The translation of A and B variant mRNAs was significantly elevated in the DKO mESCs, whereas the ΔA variant remained insensitive to 4E-BPs levels (Fig. 5*G*, *Right*). These results demonstrate that intron retention in the *Yy2* 5′-UTR, in combination with the activity of 4E-BPs, determines the outcome of *Yy2* mRNA translation. Intron retention adds an extra 117 nt to the *Yy2* 5′-UTR, increasing the complexity of its secondary structure (Fig. S6*A*) and rendering it sensitive to 4E-BP–mediated translation repression. As is consistent with the increased translation of the *Yy2* spliced variant (Fig. 5*G*), the highest expression of YY2 protein was detected in the heart and muscle tissues (Fig. S6*B*), in which the lowest degree of *Yy2* 5′-UTR intron retention is observed (Fig. 5*D* and Fig. S5*B*).

This double-layered control mechanism, consisting of the retention of the *Yy2* 5′-UTR intron by PTBP1 and suppression of translation of the resulting mRNA variant by 4E-BPs, allows the modulation of *Yy2* mRNA translation.

Discussion

Many mammalian mRNAs contain heterogeneous 5′-UTRs (48). Length, structure, and sequence elements in the 5′-UTRs strongly impact translation (49, 50). We found that the combination of alternative TSS and splicing produces four *Yy2* mRNA variants with different translation efficiencies. Thus, the relative level of each variant, in combination with 4E-BP activity, dictates the rate of YY2 protein synthesis. ESC differentiation, which is concomitant with the down-regulation of PTBP1 expression (51), triggers the splicing of the *Yy2* 5′-UTR intron. However, there is considerable variation in the extent of *Yy2* 5′-UTR intron retention among adult mouse tissues, with heart and skeletal muscle displaying the lowest rate of intron retention. Different degrees of intron retention among mouse tissues, most of which express very low levels of PTBP1 (Figs. S6*B* and S7 and Dataset S4), implies the existence of additional regulatory mechanisms that augment splicing of the *Yy2* 5′-UTR intron in heart and skeletal muscles. We also found consensus binding motifs for the MBNL1 splicing factor in the *Yy2* 5′-UTR (Fig. S5*C*). Muscleblind-like protein 1 (MBNL1) is highly expressed in cardiac and skeletal muscles (52) and is a known regulator of mRNA splicing in these tissues (53, 54). Intron retention has emerged as a widespread mechanism to regulate gene expression in different cell and tissue types as well as during stem cell differentiation (42, 55, 56). The finding that a retained intron at the 5′-UTR of *Yy2* mRNA controls its translation underscores the intricate interplay between alternative splicing and translational control (57, 58).

We established *Yy2* mRNA as a target of 4E-BP–dependent translation suppression in mESCs and demonstrated that a basal level of YY2 expression is essential for mESC survival. Similar to *Yy1*-knockout embryos, CRISPR-mediated *Yy2*-knockout embryos survived the preimplantation period, but the growth of their inner cell mass was impaired, as revealed by blastocyst outgrowth assays (Fig. 2*D*). These observations exclude the possibility of redundant functions for YY1 and YY2 in the early stages of embryonic development. The critical function of YY2 in mESCs is most likely mediated by its direct transcriptional regulation of ESC genes such as *Oct4*, *Eras*, *Tet1*, *Tet2*, and *Tdgf1*. We demonstrated that mESCs are highly sensitive to YY2 and that a modest manipulation of *Yy2* levels significantly affects the expression of pluripotency factors, ESC self-renewal, and differentiation (Figs. 2 *A*–*C* and 4 *A* and *B*). Consistent with the observed phenotype in DKO mESCs, overexpression of YY2 in WT mESCs induces down-regulation of several pluripotency factors and promotes differentiation. Although in the current study we focused on the characterization of YY2, the ribosome-profiling experiment identified several other mRNAs, such as Triggering receptor expressed on myeloid cells 2 (Triml2), Sumo1, Amigo3, Lefty, and Nodal, that display 4E-BP sensitivity. The change in translation of these additional targets in DKO mESCs could contribute to the differentiation-prone phenotype of DKO mESCs and explain the differences that may be observed between DKO mESCs and mESCs overexpressing YY2.

We documented that increased expression of YY2 directs differentiation of mouse embryoid bodies (mEBs) toward the cardiovascular lineage. The importance of YY2 in cardiomyocytes is likely not limited to early differentiation, because the heart expresses a higher level of YY2 than other tissues of adult mouse (Fig. S6*B*). This function is likely mediated by transcriptional control of the RAR pathway and multiple YY2 targets, such as *Bmp4*, *Nodal*, *Bnp*, *Mesp2*, and *Mkl1*, as evident from the ChIP-Seq analysis. Recent studies showed binding of YY1 to the promoters of highly expressed ribosomal proteins and the nuclear encoded mitochondrial membrane, enzymes, and ribosomal proteins (35) and highlighted the importance of YY1 in cardiomyocyte differentiation and heart morphogenesis (30, 31). Notably, cardiac-specific ablation of Yy1 causes severe abnormalities in the heart, indicating that YY2 in the heart does not compensate for YY1 deletion (31). Comparison of YY2 and YY1 ChIP-Seq data (Fig. 4*C* and Dataset S3) demonstrated overlapping sets of nuclear encoded mitochondrial proteins, such as the aminoacyl tRNA synthetases *Tars2*, and *Lars2*, as well as mitochondrial ribosomal proteins *Mrps18c*, *Mrpl1*, *Mrpl44*, and *Mrpl53* (Fig. 4*C* and Dataset S3). That YY2 and YY1 have both unique and overlapping target genes explains their convergent but nonredundant functions in development.

The reduced expression of several pluripotency markers (e.g., Oct4, Nanog, PRDM14, and Esrrb) in DKO mESCs and their greater tendency for differentiation (e.g., slower proliferation and a flattened morphology) resembles a “primed” state of pluripotency (59). Although the transcriptional regulatory network safeguarding the naive/primed state of pluripotency has been studied extensively, the role of posttranscriptional control mechanisms, particularly translational control, remained largely unexplored. The importance of posttranscriptional regulatory processes has been highlighted recently by the identification of the RNA-binding proteins Pum1 and Lin28 as regulators of naive/primed pluripotency (60, 61). Detailed analysis of mRNA translation therefore should provide valuable information about the role of translational control in these pluripotent states.

In summary, we have described a mechanism by which mESC self-renewal and lineage commitment are controlled via stringent regulation of YY2 expression at two stages: (*i*) by repressing the splicing of the *Yy2* 5′-UTR intron via PTBP1 and (*ii*) by suppressing the translation of the resulting mRNA variant by 4E-BP1 and -2.

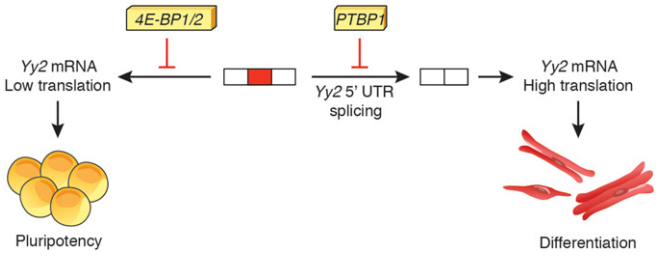

Fig. 6. Regulation of YY2 expression by splicing and mRNA translational control. A proposed model depicting the regulation of YY2 expression at two different steps: (*i*) alternative splicing (via PTBP1) and (*ii*) mRNA translation (via 4E-BP1/2). A basal level of YY2 expression is required for maintenance of mESC self-renewal, but increased translation of *Yy2* mRNA directs cardiovascular lineage commitment.

These two layers of control (Fig. 6) coalesce to limit the expression of YY2 protein to a low basal level in mESCs, thereby maintaining their self-renewal and pluripotency.

Materials and Methods

ESC Cell Culture and Differentiation. Mouse ESCs were maintained in DMEM (Wisent Inc.), 1% nonessential amino acids (Gibco), 1% L-Glutamine (Wisent Inc.), 1% sodium pyruvate (100× stock from Invitrogen), 0.1 mM β-mercaptoethanol, 15% (vol/vol) FBS, 1,000 U mouse LIF/mL (ESGRO; Millipore), penicillin (50 μg/mL), and streptomycin (50 μg/mL) and were expanded on the feeder layer or gelatin. For mESC differentiation (62), 800–2,000 mESCs were cultured for 2 d in hanging drops containing differentiation medium [DMEM, 20% (vol/vol) FBS, 1% nonessential amino acids (Gibco), 1% L-Glutamine (Wisent Inc.), penicillin (50 μg/mL), and streptomycin (50 μg/mL)]. The resulting EBs were transferred to bacteriological dishes and cultured in suspension for 3 d. Then they were plated onto gelatin-coated tissue-culture plates for the rest of the differentiation process.

Single-Guide RNA Synthesis. The DNA template for *Yy2* single-guide RNA (sgRNA) was synthesized by PCR reactions using px330 (Addgene) as a template. Two primers were used: T7-*Yy2*-sgRNA forward (5′-TTAATACGACTCACTATAGGTTCGATGGTTTGGCCTACGCGTTTTAGAGCTAGAAATAGC-3′) and sgRNA reverse (5′-AAAAGCACCGACTCGGTGCC-3′). The PCR product was purified with the PCR DNA fragments extraction kit (Geneaid) and was used as a template for sgRNA synthesis with the T7 MAXIscript kit (Ambion). The synthesized sgRNA was EtOH-precipitated and dissolved in RNase-free water.

Cytoplasmic Microinjection, Embryo Culture, and Blastocyst Outgrowth. The animal ethics committee of the McGill University approved all the animal procedures. Cas9 mRNA (50 ng/μL) (Sigma) and 50 ng/μL *Yy2*-sgRNA in 10 mM KCl were injected into CD1 zygotes in M2 medium (Zenith Biotech). Cytoplasmic injection was performed with a FemtoJet microinjector (Eppendorf) and a Cyto721 intracellular amplifier (World Precision Instruments) for the tickler's oscillation to penetrate the zygote's membrane. The injected zygotes were cultured for 4 d in KSOM drops covered with mineral oil (Zenith Biotech) in a 5% (vol/vol) CO_2 incubator at 37 °C. The zona pellucidae of the developed blastocysts were removed with acid Tyrode's solution (Millipore). The blastocysts were plated on gelatin-coated 24-well plates and were cultured 5–7 d in DMEM (Wisent) with ES-FBS (Wisent).

Cycloheximide Treatment and Hypotonic Cell Lysis. Cells were pretreated with cycloheximide (100 μg/mL) (catalog no. CYC003; BioShop Canada) for 5 min and were lysed in hypotonic buffer [5 mM Tris·HCl (pH 7.5), 2.5 mM MgCl2, 1.5 mM KCl, 1× protease inhibitor mixture (EDTA-free), 100 μg/mL cycloheximide, 2 mM DTT, 200 U/mL RNaseIn, 0.5% Triton X-100, and 0.5% sodium deoxycholate] to isolate the polysomes with centrifugation (20,000 × *g*) at 4 °C for 5 min.

Polysome Fractionation. Polysomes prepared as described in the previous paragraph (250 μg) were separated on a 10–50% (wt/vol) sucrose gradient by ultracentrifugation at 36,000 rpm for 2 h in an SW40 Ti rotor (Beckman Coulter) at 4 °C and were fractionated using an ISCO gradient fractionation system. OD at 254 nm was continuously recorded with a FOXO JR Fractionator (Teledyne ISCO).

Collection of RFPs. The ribosome profiling assay was performed as described (63), with minor modifications. Briefly, 500 μg of the ribonucleoproteins (two biological replicates, prepared as described in the section *Cycloheximide Treatment and Hypotonic Cell Lysis*) were subjected to ribosome footprinting by RNase I treatment at 4 °C for 50 min with gentle mixing. Monosomes were pelleted by ultracentrifugation in a 34% (wt/vol) sucrose cushion at 70,000 rpm for 3 h (TLA 120.2, Beckman Coulter), and RNA fragments were extracted twice with acid phenol, once with chloroform, and were precipitated with isopropanol in the presence of NaOAc and GlycoBlue (Ambion). Purified RNA was resolved on a denaturing 15% (wt/vol) polyacrylamide urea gel, and the section corresponding to 28–32 nt containing the RFPs was excised, eluted, and precipitated by isopropanol.

Random RNA Fragmentation and mRNA-Seq. Cytoplasmic RNA (150 μg) was used for mRNA-Seq analysis. Poly(A)$^+$ mRNAs were purified using magnetic oligo-dT Dynabeads (Invitrogen) according to the manufacturer's instructions. Purified RNA was eluted from the beads and mixed with an equal volume of 2× alkaline fragmentation solution (2 mM EDTA, 10 mM $Na2CO_3$, 90 mM $NaHCO_3$, pH 9.2) and incubated for 20 min at 95 °C. Fragmentation reactions were mixed with stop/precipitation solution [300 mM NaOAc (pH 5.5) and GlycoBlue], followed by isopropanol precipitation. Fragmented mRNA was size-selected on a denaturing 10% (wt/vol) polyacrylamide urea gel, and the area corresponding to 35–50 nt was excised, eluted, and precipitated with isopropanol.

ACKNOWLEDGMENTS. We thank Martin Klar, Tommy Alain, Joshua Dunn, Jelena Popic, and Ola Larsson for discussions; Serge Gueroussov, Bushra Raj, and Vinagolu Rajasekhar for reagents; Joseph Marcotrigiano for the HEK293H cell line; and Annie Sylvestre and Annik Lafrance for animal care. This work was supported by Canadian Institutes of Health Research CIHR Grants MOP-142200 (to N.S.), MOP-125885 (to V.G.), MOP-115090 (to G.B.), MOP-111197 (to Y.Y.), and MOP-14609 (to B.J.B.). S.M.J. is the recipient of a CIHR Postdoctoral fellowship. S.T. is the recipient of a Richard and Edith Strauss fellowship. U.B. is the recipient of a Human Frontier Science Program Long Term Fellowship. T.G.-P. was supported by an EMBO (European Molecular Biology Organization) Fellowship and an Ontario Institute for Regenerative Medicine Fellowship.

1. Niwa H, Miyazaki J, Smith AG (2000) Quantitative expression of Oct-3/4 defines differentiation, dedifferentiation or self-renewal of ES cells. *Nat Genet* 24(4):372–376.
2. Kopp JL, Ormsbee BD, Desler M, Rizzino A (2008) Small increases in the level of Sox2 trigger the differentiation of mouse embryonic stem cells. *Stem Cells* 26(4):903–911.
3. Sampath P, et al. (2008) A hierarchical network controls protein translation during murine embryonic stem cell self-renewal and differentiation. *Cell Stem Cell* 2(5):448–460.
4. Signer RA, Magee JA, Salic A, Morrison SJ (2014) Haematopoietic stem cells require a highly regulated protein synthesis rate. *Nature* 509(7498):49–54.
5. Blanco S, et al. (2016) Stem cell function and stress response are controlled by protein synthesis. *Nature* 534(7607):335–340.
6. Lu R, et al. (2009) Systems-level dynamic analyses of fate change in murine embryonic stem cells. *Nature* 462(7271):358–362.
7. Sonenberg N, Hinnebusch AG (2009) Regulation of translation initiation in eukaryotes: Mechanisms and biological targets. *Cell* 136(4):731–745.
8. Beretta L, Gingras AC, Svitkin YV, Hall MN, Sonenberg N (1996) Rapamycin blocks the phosphorylation of 4E-BP1 and inhibits cap-dependent initiation of translation. *EMBO J* 15(3):658–664.
9. Pelletier J, Graff J, Ruggero D, Sonenberg N (2015) Targeting the eIF4F translation initiation complex: A critical nexus for cancer development. *Cancer Res* 75(2):250–263.
10. Brunn GJ, et al. (1997) Phosphorylation of the translational repressor PHAS-I by the mammalian target of rapamycin. *Science* 277(5322):99–101.
11. Hara K, et al. (1997) Regulation of eIF-4E BP1 phosphorylation by mTOR. *J Biol Chem* 272(42):26457–26463.
12. Pause A, et al. (1994) Insulin-dependent stimulation of protein synthesis by phosphorylation of a regulator of 5′-cap function. *Nature* 371(6500):762–767.
13. Hartman NW, et al. (2013) mTORC1 targets the translational repressor 4E-BP2, but not S6 kinase 1/2, to regulate neural stem cell self-renewal in vivo. *Cell Reports* 5(2):433–444.
14. Signer RA, et al. (2016) The rate of protein synthesis in hematopoietic stem cells is limited partly by 4E-BPs. *Genes Dev* 30(15):1698–1703.
15. Koromilas AE, Lazaris-Karatzas A, Sonenberg N (1992) mRNAs containing extensive secondary structure in their 5′ non-coding region translate efficiently in cells overexpressing initiation factor eIF-4E. *EMBO J* 11(11):4153–4158.
16. Bhat M, et al. (2015) Targeting the translation machinery in cancer. *Nat Rev Drug Discov* 14(4):261–278.
17. Tahmasebi S, et al. (2014) Multifaceted regulation of somatic cell reprogramming by mRNA translational control. *Cell Stem Cell* 14(5):606–616.
18. Dowling RJ, et al. (2010) mTORC1-mediated cell proliferation, but not cell growth, controlled by the 4E-BPs. *Science* 328(5982):1172–1176.

19. Ingolia NT, Ghaemmaghami S, Newman JR, Weissman JS (2009) Genome-wide analysis in vivo of translation with nucleotide resolution using ribosome profiling. *Science* 324(5924):218–223.
20. Olshen AB, et al. (2013) Assessing gene-level translational control from ribosome profiling. *Bioinformatics* 29(23):2995–3002.
21. Nguyen N, Zhang X, Olashaw N, Seto E (2004) Molecular cloning and functional characterization of the transcription factor YY2. *J Biol Chem* 279(24):25927–25934.
22. Kim JD, Faulk C, Kim J (2007) Retroposition and evolution of the DNA-binding motifs of YY1, YY2 and REX1. *Nucleic Acids Res* 35(10):3442–3452.
23. Rogers MB, Hosler BA, Gudas LJ (1991) Specific expression of a retinoic acid-regulated, zinc-finger gene, Rex-1, in preimplantation embryos, trophoblast and spermatocytes. *Development* 113(3):815–824.
24. Luo C, Lu X, Stubbs L, Kim J (2006) Rapid evolution of a recently retroposed transcription factor YY2 in mammalian genomes. *Genomics* 87(3):348–355.
25. Vella P, Barozzi I, Cuomo A, Bonaldi T, Pasini D (2012) Yin Yang 1 extends the Myc-related transcription factors network in embryonic stem cells. *Nucleic Acids Res* 40(8): 3403–3418.
26. Donohoe ME, et al. (1999) Targeted disruption of mouse Yin Yang 1 transcription factor results in peri-implantation lethality. *Mol Cell Biol* 19(10):7237–7244.
27. Onder TT, et al. (2012) Chromatin-modifying enzymes as modulators of reprogramming. *Nature* 483(7391):598–602.
28. Thoreen CC, et al. (2012) A unifying model for mTORC1-mediated regulation of mRNA translation. *Nature* 485(7396):109–113.
29. Donohoe ME, Zhang LF, Xu N, Shi Y, Lee JT (2007) Identification of a Ctcf cofactor, Yy1, for the X chromosome binary switch. *Mol Cell* 25(1):43–56.
30. Gregoire S, et al. (2013) Essential and unexpected role of Yin Yang 1 to promote mesodermal cardiac differentiation. *Circ Res* 112(6):900–910.
31. Beketaev I, et al. (2015) Critical role of YY1 in cardiac morphogenesis. *Dev Dyn* 244(5): 669–680.
32. Sigova AA, et al. (2015) Transcription factor trapping by RNA in gene regulatory elements. *Science* 350(6263):978–981.
33. Wobus AM, et al. (1997) Retinoic acid accelerates embryonic stem cell-derived cardiac differentiation and enhances development of ventricular cardiomyocytes. *J Mol Cell Cardiol* 29(6):1525–1539.
34. Pan J, Baker KM (2007) Retinoic acid and the heart. *Vitam Horm* 75:257–283.
35. Chen L, et al. (2010) Genome-wide analysis of YY2 versus YY1 target genes. *Nucleic Acids Res* 38(12):4011–4026.
36. Klar M (2010) It is not necessarily YY1–the frequently forgotten Yin-Yang-2 transcription factor. *Proc Natl Acad Sci USA* 107(52):E190–author reply E191.
37. Klar M, Bode J (2005) Enhanceosome formation over the beta interferon promoter underlies a remote-control mechanism mediated by YY1 and YY2. *Mol Cell Biol* 25(22):10159–10170.
38. Lee SH, et al. (2016) Yin-Yang 1 and Yin-Yang 2 exert opposing effects on the promoter activity of interleukin 4. *Arch Pharm Res* 39(4):547–554.
39. Wang L, Brown SJ (2006) BindN: A web-based tool for efficient prediction of DNA and RNA binding sites in amino acid sequences. *Nucleic Acids Res* 34(Web Server issue): W243–248.
40. Vinckenbosch N, Dupanloup I, Kaessmann H (2006) Evolutionary fate of retroposed gene copies in the human genome. *Proc Natl Acad Sci USA* 103(9):3220–3225.
41. Fablet M, Bueno M, Potrzebowski L, Kaessmann H (2009) Evolutionary origin and functions of retrogene introns. *Mol Biol Evol* 26(9):2147–2156.
42. Braunschweig U, et al. (2014) Widespread intron retention in mammals functionally tunes transcriptomes. *Genome Res* 24(11):1774–1786.
43. Paz I, Kosti I, Ares M, Jr, Cline M, Mandel-Gutfreund Y (2014) RBPmap: A web server for mapping binding sites of RNA-binding proteins. *Nucleic Acids Res* 42(Web Server issue):W361–W367.
44. Oberstrass FC, et al. (2005) Structure of PTB bound to RNA: Specific binding and implications for splicing regulation. *Science* 309(5743):2054–2057.
45. Shibayama M, et al. (2009) Polypyrimidine tract-binding protein is essential for early mouse development and embryonic stem cell proliferation. *FEBS J* 276(22):6658–6668.
46. Suckale J, et al. (2011) PTBP1 is required for embryonic development before gastrulation. *PLoS One* 6(2):e16992.
47. Colina R, et al. (2008) Translational control of the innate immune response through IRF-7. *Nature* 452(7185):323–328.
48. Melé M, et al.; GTEx Consortium (2015) Human genomics. The human transcriptome across tissues and individuals. *Science* 348(6235):660–665.
49. Floor SN, Doudna JA (2016) Tunable protein synthesis by transcript isoforms in human cells. *eLife* 5:e10921.
50. de Klerk E, t'Hoen PA (2015) Alternative mRNA transcription, processing, and translation: Insights from RNA sequencing. *Trends Genet* 31(3):128–139.
51. Linares AJ, et al. (2015) The splicing regulator PTBP1 controls the activity of the transcription factor Pbx1 during neuronal differentiation. *eLife* 4:e09268.
52. Miller JW, et al. (2000) Recruitment of human muscleblind proteins to (CUG)(n) expansions associated with myotonic dystrophy. *EMBO J* 19(17):4439–4448.
53. Kino Y, et al. (2009) MBNL and CELF proteins regulate alternative splicing of the skeletal muscle chloride channel CLCN1. *Nucleic Acids Res* 37(19):6477–6490.
54. Han H, et al. (2013) MBNL proteins repress ES-cell-specific alternative splicing and reprogramming. *Nature* 498(7453):241–245.
55. Wong JJ, et al. (2013) Orchestrated intron retention regulates normal granulocyte differentiation. *Cell* 154(3):583–595.
56. Yap K, Lim ZQ, Khandelia P, Friedman B, Makeyev EV (2012) Coordinated regulation of neuronal mRNA steady-state levels through developmentally controlled intron retention. *Genes Dev* 26(11):1209–1223.
57. Sterne-Weiler T, et al. (2013) Frac-seq reveals isoform-specific recruitment to polyribosomes. *Genome Res* 23(10):1615–1623.
58. Maslon MM, Heras SR, Bellora N, Eyras E, Cáceres JF (2014) The translational landscape of the splicing factor SRSF1 and its role in mitosis. *eLife* 3:e02028.
59. Nichols J, Smith A (2009) Naive and primed pluripotent states. *Cell Stem Cell* 4(6): 487–492.
60. Leeb M, Dietmann S, Paramor M, Niwa H, Smith A (2014) Genetic exploration of the exit from self-renewal using haploid embryonic stem cells. *Cell Stem Cell* 14(3): 385–393.
61. Zhang J, et al. (2016) LIN28 Regulates Stem Cell Metabolism and Conversion to Primed Pluripotency. *Cell Stem Cell* 19(1):66–80.
62. Wobus AM, Guan K, Yang HT, Boheler KR (2002) Embryonic stem cells as a model to study cardiac, skeletal muscle, and vascular smooth muscle cell differentiation. *Methods Mol Biol* 185:127–156.
63. Ingolia NT, Brar GA, Rouskin S, McGeachy AM, Weissman JS (2012) The ribosome profiling strategy for monitoring translation in vivo by deep sequencing of ribosome-protected mRNA fragments. *Nat Protoc* 7(8):1534–1550.
64. Wiederschain D, et al. (2009) Single-vector inducible lentiviral RNAi system for oncology target validation. *Cell Cycle* 8(3):498–504.
65. Thomsen S, Anders S, Janga SC, Huber W, Alonso CR (2010) Genome-wide analysis of mRNA decay patterns during early Drosophila development. *Genome Biol* 11(9):R93.
66. Bolger AM, Lohse M, Usadel B (2014) Trimmomatic: A flexible trimmer for Illumina sequence data. *Bioinformatics* 30(15):2114–2120.
67. Zhang Y, et al. (2008) Model-based analysis of ChIP-Seq (MACS). *Genome Biol* 9(9):R137.
68. Heinz S, et al. (2010) Simple combinations of lineage-determining transcription factors prime cis-regulatory elements required for macrophage and B cell identities. *Mol Cell* 38(4):576–589.
69. Kent WJ, et al. (2002) The human genome browser at UCSC. *Genome Res* 12(6): 996–1006.
70. Barbosa-Morais NL, et al. (2012) The evolutionary landscape of alternative splicing in vertebrate species. *Science* 338(6114):1587–1593.
71. Gueroussov S, et al. (2015) An alternative splicing event amplifies evolutionary differences between vertebrates. *Science* 349(6250):868–873.